

# One-Dimensional Cobalt Diphosphonates Exhibiting Weak Ferromagnetism and Field-Induced Magnetic Transitions

Li-Min Zheng,<sup>\*†</sup> Song Gao,<sup>‡</sup> Ping Yin,<sup>†</sup> and Xin-Quan Xin<sup>†</sup>

State Key Laboratory of Coordination Chemistry, Coordination Chemistry Institute, Nanjing University, Nanjing 210093, P. R. China, and State Key Laboratory of Rare Earth Materials Chemistry and Applications, College of Chemistry and Molecular Engineering, Peking University, Beijing 100871, P. R. China

Received June 3, 2003

This paper reports two new cobalt phosphonate compounds  $[\text{NH}_3(\text{CH}_2)_n\text{NH}_3]\text{Co}_2(\text{hedpH})_2 \cdot 2\text{H}_2\text{O}$  [ $n = 4$  (**1**),  $5$  (**2**)], where hedp is (1-hydroxyethylidene)diphosphonate  $[\text{CH}_3\text{C}(\text{OH})(\text{PO}_3)_2]$ . Both contain ladderlike chains with the same composition  $\{\text{Co}_2(\text{hedpH})_2\}_n^{2n-}$ , where edge-shared  $\{\text{CoO}_6\}$  octahedra are each bridged by O–P–O units. The chains are linked by very strong hydrogen bonds to form a three-dimensional open network with channels in which the diammonium counterions and lattice water reside. Magnetic studies reveal dominant antiferromagnetic interactions between the Co centers within the chain in both compounds. The field dependent magnetization confirms the occurrence of the field-induced magnetic transitions, with the critical fields ca. 25 kOe for **1** and 27.5 kOe for **2**, respectively. In the case of compound **2**, weak ferromagnetism is also observed at very low temperatures, possibly arising from spin canting of the antiferromagnetically coupled Co(II) ions in the chain. Crystal data: **1**, monoclinic,  $P2_1/c$ ,  $a = 5.4868(8)$ ,  $b = 12.9116(18)$ , and  $c = 15.251(2)$  Å,  $\beta = 98.843(2)^\circ$ ,  $V = 1067.6(3)$  Å<sup>3</sup>,  $Z = 2$ ; **2**, monoclinic,  $P2_1/c$ ,  $a = 5.4757(7)$ ,  $b = 12.7740(16)$ , and  $c = 15.794(2)$  Å,  $\beta = 98.797(2)^\circ$ ,  $V = 1091.7(2)$  Å<sup>3</sup>,  $Z = 2$ .

## Introduction

Low-dimensional magnetic materials especially the quantum spin systems are of considerable current interest in material science.<sup>1–7</sup> It has been well-known that many metal phosphonate compounds exhibit layered or pillared layered structures where the inorganic layers are separated by organic moieties.<sup>8</sup> Other structure types have also been reported,

among which some are chain structures.<sup>8c,9</sup> Interesting magnetic properties such as weak ferromagnetism and metamagnetism have been observed in some compounds.<sup>10–16</sup>

\* To whom correspondence should be addressed. E-mail: lmzheng@netra.nju.edu.cn. Fax: +86-25-3314502 or 3317761.

<sup>†</sup> Nanjing University.

<sup>‡</sup> Peking University.

(1) Sachdev, S. *Science* **2000**, *288*, 475.

(2) Tandon, K.; Lal, S.; Pati, S. K.; Ramasesha, S.; Sen, D. *Phys. Rev. B* **1999**, *59*, 396.

(3) Carlin, R. L. *Magnetochemistry*; Springer-Verlag: Berlin, Heidelberg, 1986.

(4) Chaboussant, G.; Crowell, P. A.; Levy, L. P.; Piovesana, O.; Madouri, A.; Maily, D. *Phys. Rev. B* **1997**, *55*, 3046.

(5) Watson, B. C.; Kotov, V. N.; Meisel, M. W.; Hall, D. W.; Granroth, G. E.; Montfrooij, W. T.; Nagler, S. E.; Jensen, D. A.; Backov, R.; Petruska, M. A.; Fanucci, G. E.; Talham, D. R. *Phys. Rev. Lett.* **2001**, *86*, 5168.

(6) Azuma, M.; Hiroi, Z.; Takano, M.; Ishida, K.; Kitaoka, Y. *Phys. Rev. Lett.* **1994**, *73*, 3463.

(7) Eccleston, R. S.; Barnes, T.; Brody, J.; Johnson, J. W. *Phys. Rev. Lett.* **1994**, *73*, 2626.

(8) For example: (a) Cao, G.; Hong, H.-G.; Mallouk, T. E. *Acc. Chem. Res.* **1992**, *25*, 420. (b) Alberti, G. *Comprehensive Supramolecular Chemistry*; Lehn, J. M., Ed.; Pergamon Elsevier Science, Ltd.: Oxford, U.K., 1996; Vol. 7. (c) Clearfield, A. *Progress in Inorganic Chemistry*; Karlin, K. D., Ed.; John Wiley & Sons: New York, 1998; Vol. 47, pp 371–510 and references therein.

(9) For example: (a) Mao, J. G.; Wang Z. K.; Clearfield, A. *Inorg. Chem.* **2002**, *41*, 6106. (b) Sharma, C. V. K.; Clearfield, A.; Cabeza, A.; Aranda, M. A. G.; Bruque, S. *J. Am. Chem. Soc.* **2001**, *123*, 2885. (c) Barthelet, K.; Nogues, M.; Riou, D.; Ferey, G. *Chem. Mater.* **2002**, *14*, 4910. (d) Serre, C.; Ferey, G. *J. Mater. Chem.* **2002**, *12*, 2367. (e) Finn, R. C.; Zubieta, J.; Haushalter, R. C. *Prog. Inorg. Chem.* **2003**, *51*, 421. (f) Finn, R. C.; Burkholder, E.; Zubieta, J. *Chem. Commun.* **2001**, 1852. (g) Fredoueil, F.; Evain, M.; Massiot, D.; Bujolis-Doeuff, M.; Janvier, P.; Clearfield, A.; Bujoli, B. *J. Chem. Soc., Dalton Trans.* **2002**, 1508. (h) Stock, N.; Stucky, G. D.; Cheetham, A. K. *Chem. Commun.* **2000**, 2277. (i) Ngo, H. L.; Lin, W. B. *J. Am. Chem. Soc.* **2002**, *124*, 14298. (j) Evans, O. R.; Ngo, H. L.; Lin, W. B. *J. Am. Chem. Soc.* **2001**, *123*, 10395. (k) Harvey, H. G.; Teat, S. J.; Tang, C. C.; Cranswick, L. M.; Attfield, M. P. *Inorg. Chem.* **2003**, *42*, 2428. (l) Jankovics, H.; Daskalakis, M.; Raptopoulou, C. P.; Terzis, A.; Tangoulis, V.; Giapintzakis, J.; Kiss, T.; Salifoglou, A. *Inorg. Chem.* **2002**, *41*, 3366. (m) Lohse, D. L.; Sevov, S. C. *Angew. Chem., Int. Ed. Engl.* **1997**, *36*, 1619.

(10) Gao, Q. M.; Guillou, N.; Nogues, M.; Cheetham, A. K.; Ferey, G. *Chem. Mater.* **1999**, *11*, 2937.

On the basis of (1-hydroxyethylidene)diphosphonate [hedp,  $\text{CH}_3\text{C}(\text{OH})(\text{PO}_3)_2$ ], where the two phosphorus groups are separated by a methyl group, we have synthesized a series of M–hedp compounds with chain structures.<sup>17–20</sup> Compounds containing ladderlike motifs of  $\{\text{M}_2(\text{hedpH})_2\}_n^{2n-}$  (M = Mn, Fe, Co) are of particular interest because they provide new systems of low-dimensional materials for magnetic studies. In this paper, we report the magnetic properties of two new cobalt compounds with similar ladderlike structures.

## Experimental Section

**Materials and Methods.** All the starting materials were reagent grade used as purchased. The 50% aqueous solution of (1-hydroxyethylidene)diphosphonic acid (hedpH<sub>4</sub>) was purchased from Nanjing Shuguang Chemical Factory of China. The elemental analyses were performed on a PE 240C elemental analyzer. The infrared spectra were recorded on a Nicolet 170SX FT-IR spectrometer with pressed KBr pellets. The magnetic susceptibility measurements for **1** and **2** were carried out on polycrystalline samples (29.8 mg for **1** and 32.6 mg for **2**) using a MagLab System 2000 magnetometer in a magnetic field up to 7 T. Diamagnetic corrections were estimated from Pascal's constants.<sup>21</sup>

**Synthesis of  $[\text{NH}_3(\text{CH}_2)_4\text{NH}_3]\text{Co}_2(\text{hedpH})_2 \cdot 2\text{H}_2\text{O}$ , **1**.** A mixture of  $\text{CoCl}_2 \cdot 6\text{H}_2\text{O}$  (1 mmol, 0.2390 g), 50% hedpH<sub>4</sub> (1 cm<sup>3</sup>), and H<sub>2</sub>O (8 cm<sup>3</sup>), adjusted with 1,4-butylenediamine to pH = 4.83, was treated hydrothermally at 140 °C for 45 h. Purple red needlelike crystals were produced as a single phase, judged by the powder X-ray pattern in comparison with the pattern deduced from single-crystal data. Yield: 89% based on Co. Anal. Found: C, 16.05; H, 4.87; N, 5.47. Calcd for  $\text{C}_8\text{H}_{28}\text{Co}_2\text{N}_2\text{O}_{16}\text{P}_4$ : C, 14.77; H, 4.31; N, 4.31. IR (KBr, cm<sup>-1</sup>): 3419 s, 3351 s, 3007 s (br), 2937 s, 2889 s, 2767 s, 2294 w, 2049 w, 1681 m, 1631 m, 1553 s, 1485 m, 1430 m, 1134 vs, 1001 m, 920 s, 784 m, 671 w, 576 s, 504 w, 473 vw.

**Synthesis of  $[\text{NH}_3(\text{CH}_2)_5\text{NH}_3]\text{Co}_2(\text{hedpH})_2 \cdot 2\text{H}_2\text{O}$ , **2**.** The hydrothermal treatment of a mixture of  $\text{CoCl}_2 \cdot 6\text{H}_2\text{O}$  (1 mmol, 0.2370 g), 50% hedpH<sub>4</sub> (1 cm<sup>3</sup>), NaF (1 mmol, 0.0464 g), and H<sub>2</sub>O (8 cm<sup>3</sup>), adjusted by 1,5-diaminopentane to pH = 4.41, in a Teflon-lined autoclave at 140 °C for 49 h resulted in the formation of the purple red needlelike crystals of compound **2** as a monophasic material. Yield: 71% based on Co. Anal. Found: C, 17.37; H, 4.62; N, 5.09. Calcd for  $\text{C}_9\text{H}_{30}\text{Co}_2\text{N}_2\text{O}_{16}\text{P}_4$ : C, 16.27; H, 4.52; N, 4.22.

**Table 1.** Crystallographic Data

param	1	2
formula	$\text{C}_8\text{H}_{28}\text{Co}_2\text{N}_2\text{O}_{16}\text{P}_4$	$\text{C}_9\text{H}_{30}\text{Co}_2\text{N}_2\text{O}_{16}\text{P}_4$
$M_r$	650.06	664.09
cryst system	monoclinic	monoclinic
space group	$P2_1/c$	$P2_1/c$
$a/\text{Å}$	5.4868(8)	5.4757(7)
$b/\text{Å}$	12.9116(18)	12.7740(16)
$c/\text{Å}$	15.251(2)	15.794(2)
$\beta/\text{deg}$	98.843(2)	98.797(2)
$V/\text{Å}^3$	1067.6(3)	1091.7(2)
Z	2	2
$D_c/\text{g cm}^{-3}$	2.022	2.020
$F(000)$	664	680
$\mu(\text{Mo K}\alpha)/\text{cm}^{-1}$	19.35	18.95
goodness of fit on $F^2$	0.924	1.136
R1, wR2 <sup>a</sup> [ $I > 2\sigma(I)$ ]	0.0352, 0.0715	0.0427, 0.1019
R1, wR2 <sup>a</sup> (all data)	0.0493, 0.0742	0.0539, 0.1075
$(\Delta\rho)_{\text{max}}, (\Delta\rho)_{\text{min}}/\text{e Å}^{-3}$	0.465, -0.391	0.934, -0.508

$$^a R1 = \sum ||F_o| - |F_c|| / \sum |F_o|. \quad wR2 = [\sum w(F_o^2 - F_c^2)^2 / \sum w(F_o^2)^2]^{1/2}.$$

IR (KBr, cm<sup>-1</sup>): 3419 vs, 3273–2780 s (br), 1678 m, 1627 m, 1569 w, 1496 m, 1413 w, 1133 vs, 1005 m, 921 s, 788 m, 673 w, 571 s, 499 vw, 467 w.

**X-ray Crystallographic Analysis.** Crystals with dimensions 0.40 × 0.15 × 0.15 mm for **1** and 0.40 × 0.15 × 0.15 mm for **2** were selected for indexing and intensity data collection at 293(2) K on a Bruker SMART APEX CCD diffractometer with monochromated Mo K $\alpha$  ( $\lambda = 0.71073 \text{ Å}$ ) radiation. A hemisphere of data (1271 frames at 5 cm detector distance) was collected using a narrow-frame method with scan widths of 0.30° in  $\omega$  and an exposure time of 10 s/frame for **1** and 20 s/frame for **2**. The data were integrated using the Siemens SAINT program,<sup>22</sup> with the intensities corrected for the Lorentz factor, polarization, air absorption, and absorption due to variation in the path length through the detector faceplate. An empirical absorption was applied for both compounds.

The structures were solved by direct methods and refined on  $F^2$  by full-matrix least squares using SHELXTL.<sup>23</sup> All the non-hydrogen atoms except the disordered C atoms in **2** were refined anisotropically. The disordered C and all the hydrogen atoms were refined isotropically. The hydrogen atoms attached to the disordered C atoms were not located. Selected crystallographic data and structure determination parameters are given in Table 1, and selected bond lengths and angles in Table 2.

## Results and Discussion

**Crystal Structures.** Compounds **1** and **2** are isostructural. Their structures are closely related to those of compounds  $[\text{NH}_3(\text{CH}_2)_n\text{NH}_3]\text{M}_2(\text{hedpH})_2 \cdot 2\text{H}_2\text{O}$  (M = Fe, Mn, Zn;  $n = 4, 5$ ).<sup>17–19</sup> They contain similar  $\{\text{Co}_2(\text{hedpH})_2\}_n$  double chains in which edge-shared  $\text{CoO}_6$  octahedra are bridged by O–P–O units (Figure 1). Each double chain in **1** and **2** is connected to its four equivalent neighbors through very strong hydrogen bonds  $[\text{O}(3) \cdots \text{O}(6)]: 2.428(3)$  for **1**, 2.433–(4) Å for **2**], thus forming a three-dimensional open network with channels generated along [100] directions. The  $[\text{NH}_3(\text{CH}_2)_n\text{NH}_3]^{2+}$  ( $n = 4, 5$ ) cations and lattice water reside in the channels (Figures 2 and 3).

Although the overall structures of compounds **1** and **2** are analogous, the counterions with different alkyl lengths clearly

- (11) (a) Bujoli, B.; Pena, O.; Palvadeau, P.; Le Bideau, J.; Payen, C.; Rouxel, J. *Chem. Mater.* **1993**, *5*, 583; (b) Bellitto, C.; Federici, F.; Altomare, A.; Rizzi, R.; Ibrahim, S. A. *Inorg. Chem.* **2000**, *39*, 1803. (c) Bellitto, C.; Federici, F. *Inorg. Chem.* **2002**, *41*, 709.
- (12) Bellitto, C.; Federici, F.; Ibrahim, S. A. *Chem. Commun.* **1996**, 759.
- (13) Carling, S. G.; Visser, D.; Kremer, R. K. *J. Solid State Chem.* **1993**, *106*, 111.
- (14) Rabu, P.; Janvier, P.; Bujoli, B. *J. Mater. Chem.* **1999**, *9*, 1323.
- (15) Gutschke, S. O. H.; Price, D. J.; Powell, A. K.; Wood, P. T. *Angew. Chem., Int. Ed.* **1999**, *38*, 1088.
- (16) Yin, P.; Gao, S.; Zheng, L.-M.; Wang, Z.; Xin, X.-Q. *Chem. Commun.* **2003**, 1076. Zheng, L.-M.; Gao, S.; Song, H.-H.; Decurtins, S.; Jacobson, A. J.; Xin, X.-Q. *Chem. Mater.* **2002**, *14*, 3143.
- (17) Zheng, L.-M.; Song, H.-H.; Lin, C.-H.; Wang, S.-L.; Hu, Z.; Yu, Z.; Xin, X.-Q. *Inorg. Chem.* **1999**, *38*, 4618. Song, H.-H.; Zheng, L.-M.; Zhu, G.; Shi, Z.; Feng, S.; Gao, S.; Xin, X.-Q. *Chin. J. Inorg. Chem.* **2002**, *18*, 67.
- (18) Song, H.-H.; Yin, P.; Zheng, L.-M.; Korp, J. D.; Jacobson, A. J.; Xin, X.-Q. *J. Chem. Soc., Dalton Trans.* **2002**, 2752.
- (19) Song, H.-H.; Zheng, L.-M.; Wang, Z.; Yan, C.-H.; Xin, X.-Q. *Inorg. Chem.* **2001**, *40*, 5024.
- (20) Yin, P.; Gao, S.; Zheng, L.-M.; Xin, X.-Q. *Chem. Mater.* **2003**, *15*, 3233.
- (21) Kahn, O. *Molecular Magnetism*; VCH Publishers: New York, 1993.

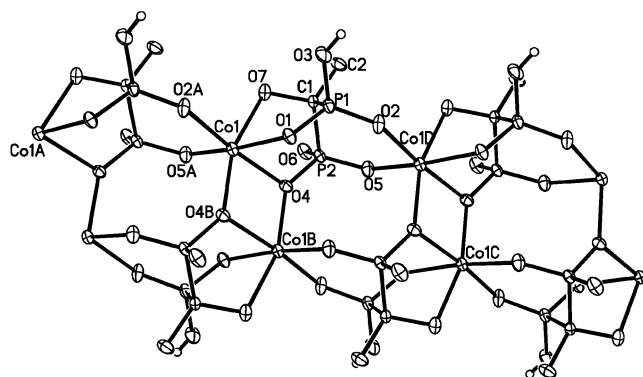
(22) SAINT, Program for Data Extraction and Reduction; Siemens Analytical X-ray Instruments Inc.: Madison, WI, 1994–1996.

(23) Sheldrick, G. M. SHELXTL PC, version 5; Siemens Analytical X-ray Instruments Inc.: Madison, WI, 1995.

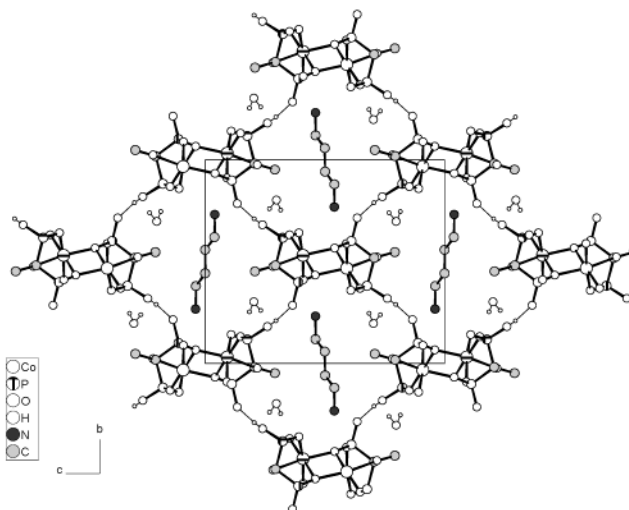
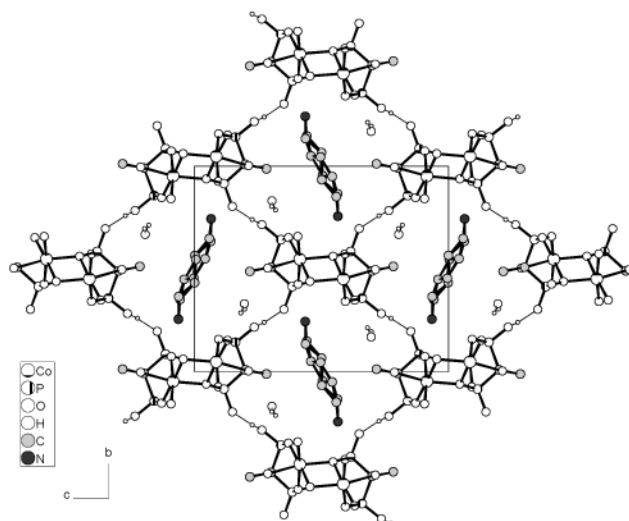
**Table 2.** Selected Bond Lengths (Å) and Angles (deg) for **1** and **2**<sup>a</sup>

	<b>1</b>	<b>2</b>
Co(1)—O(5A)	2.045(2)	2.035(3)
Co(1)—O(1)	2.080(2)	2.062(3)
Co(1)—O(2A)	2.123(2)	2.109(3)
Co(1)—O(4)	2.265(2)	2.279(3)
Co(1)—O(4B)	2.046(2)	2.052(3)
Co(1)—O(7)	2.201(2)	2.242(3)
P(1)—O(1)	1.517(2)	1.513(3)
P(1)—O(2)	1.508(2)	1.504(3)
P(1)—O(3)	1.538(2)	1.536(3)
P(2)—O(4)	1.524(2)	1.517(3)
P(2)—O(5)	1.507(2)	1.500(3)
P(2)—O(6)	1.539(2)	1.539(3)
O(5A)—Co(1)—O(4B)	96.63(8)	95.12(11)
O(5A)—Co(1)—O(1)	170.49(8)	170.49(11)
O(4B)—Co(1)—O(1)	91.30(8)	92.51(11)
O(5A)—Co(1)—O(2A)	91.14(8)	90.67(11)
O(4B)—Co(1)—O(2A)	101.58(8)	103.92(11)
O(1)—Co(1)—O(2A)	92.40(8)	92.99(11)
O(5A)—Co(1)—O(7)	90.45(8)	90.45(11)
O(4B)—Co(1)—O(7)	159.80(8)	157.43(11)
O(1)—Co(1)—O(7)	80.36(8)	80.36(10)
O(2A)—Co(1)—O(7)	97.16(8)	97.85(11)
O(5A)—Co(1)—O(4)	93.12(8)	92.01(10)
O(4B)—Co(1)—O(4)	81.21(8)	79.59(11)
O(1)—Co(1)—O(4)	82.89(8)	83.79(10)
O(2A)—Co(1)—O(4)	174.61(7)	175.37(10)
O(7)—Co(1)—O(4)	79.53(7)	78.37(10)
Co(1B)—O(4)—Co(1)	98.79(8)	100.41(11)
P(1)—O(1)—Co(1)	117.70(12)	118.45(15)
P(1)—O(2)—Co(1C)	134.43(12)	135.09(17)
P(2)—O(4)—Co(1B)	142.26(12)	140.02(17)
P(2)—O(4)—Co(1)	114.85(11)	115.07(14)
P(2)—O(5)—Co(1C)	134.95(13)	135.83(17)
C(1)—O(7)—Co(1)	105.63(15)	104.5(2)

<sup>a</sup> Symmetry transformations used to generate equivalent atoms: A,  $x + 1, y, z$ ; B,  $-x + 2, -y + 1, -z + 1$ ; C,  $x - 1, y, z$ .

**Figure 1.** Fragment of the chain with atomic labeling scheme (50% probability) in **1**.

pose influences on their structures. A close examination on their bond lengths and angles within the  $\{\text{Co}_2(\text{hedpH})_2\}_n$  double chain reveals that significant changes are found for the O—Co—O bond angles in which the bridging phosphonate oxygen [ $\mu$ -O(4)] is involved. For example, the Co(1)—O(4)—Co(1B) angles are  $98.79(8)^\circ$  in **1** and  $100.46(14)^\circ$  in **2**, respectively. The Co—O and P—O bond lengths remain nearly unchanged (Table 2). The Co $\cdots$ Co distances within the double chain are only slightly different in both cases. The Co $\cdots$ Co distances over the  $\mu$ -O(4) bridge are 3.276 and 3.236 Å for **1** and **2**, respectively. Those over the O—P—O unit along the rail and the diagonal are 5.487 and 4.867 Å for **1** and 5.464 and 4.865 Å for **2**, respectively (Figure 1).

**Figure 2.** Structure of **1** viewed along the  $a$ -axis.**Figure 3.** Structure of **2** viewed along the  $a$ -axis.

Between the double chains, there exist very strong hydrogen bonds. Although the O(3) $\cdots$ O(6) separation is essentially constant, the P—O $\cdots$ O angle increases distinctly from  $136.1^\circ$  in **1** to  $138.9^\circ$  in **2**. The same trend was observed in the cases of the Mn analogues.<sup>18</sup> In contrast to the Mn compounds, however, the  $b$  axis, which is roughly parallel to the chain of diammonium cation, is slightly shortened when diammoniopentane in **2** (12.774 Å) replaces diammoniobutane in **1** (12.912 Å), while the  $c$  axis, which is almost perpendicular to the cation chain, is lengthened from 15.251 Å (for **1**) to 15.794 Å (for **2**). This may be explained by the fact that the diammoniopentane is heavily disordered and contorted to fit into the channel. The overall unit cell volume is expanded from compound **1** to **2** as expected (Table 1).

**Magnetic Properties.** Figure 4 shows the temperature-dependent molar magnetic susceptibilities of **1** at various external fields. At 10 kOe, the room-temperature effective magnetic moment per Co ( $5.43 \mu_B$ ) is much higher than the expected spin-only value for spin  $S = 3/2$  ( $3.87 \mu_B$ ), attributed to the orbital contribution of Co(II) ion. The susceptibility data obey the Curie–Weiss law in the temperature range 25–300 K with a Weiss constant  $-13.1$  K (Figure S1,

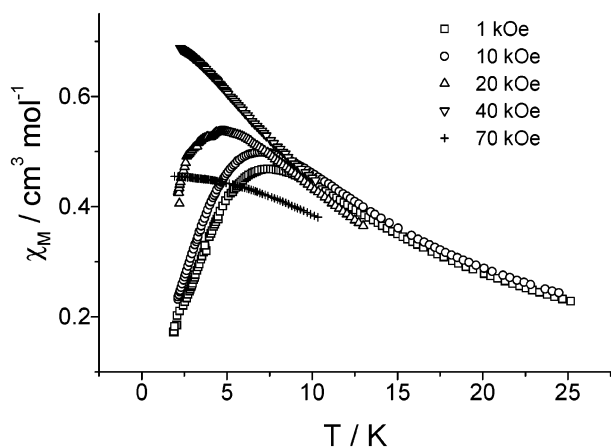
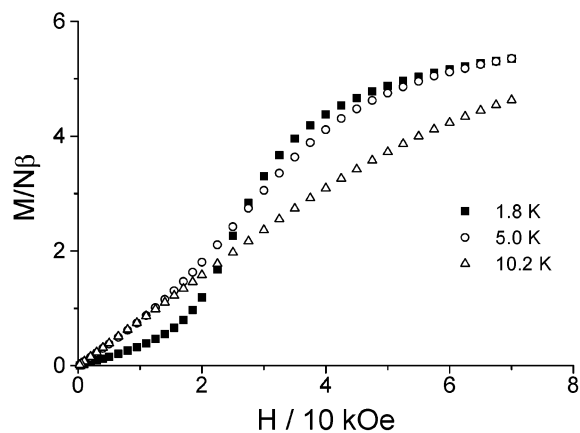


**Figure 4.**  $\chi_M$  vs  $T$  plots for **1** at different external fields.

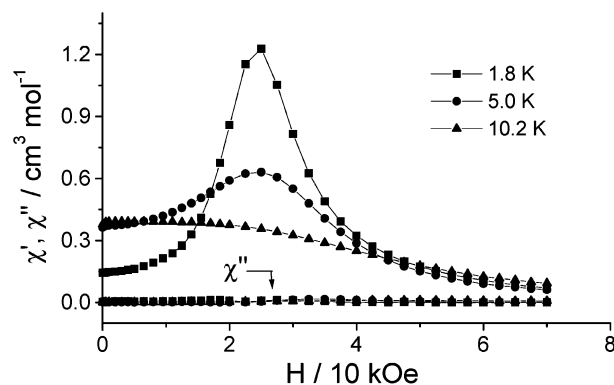
Supporting Information). The negative Weiss constant indicates a dominant antiferromagnetic interaction between the magnetic centers. The rounded peak appearing around 7 K in the  $\chi_M$  vs  $T$  curve is typical for a low-dimensional antiferromagnet. Below 7 K,  $\chi_M$  drops sharply toward zero, suggesting that the ground state of the system is  $S = 0$ . When the external field is high ( $\geq 40$  kOe), the peak in the  $\chi_M$  vs  $T$  curves disappears, suggesting the occurrence of a field-induced magnetic transition.

A low-dimensional antiferromagnet is not unexpected from the structure of compound **1** where ladderlike chains of  $\{\text{Co}_2(\text{hedpH})_2\}_n$  are interconnected by strong hydrogen bonds. Considering that the shortest  $\text{Co}\cdots\text{Co}$  distance between the chains is 8.04 Å, the antiferromagnetic exchange coupling should be mainly propagated between the Co(II) centers within the ladderlike chain through  $\mu$ -O and/or O–P–O bridges (Figure 1). As the  $\text{Co}\cdots\text{Co}$  distance over the  $\mu$ -O(4) bridge (3.276 Å) is much shorter than those over the O–P–O bridges along the leg (5.487 Å) and the diagonal (4.867 Å), the exchange through the  $\mu$ -O(4) bridge should be dominant. A theoretical analysis based on an isotropic dimer model of spin  $S = 3/2$ , however, is not successful due to the orbital contribution of the Co(II) ions.

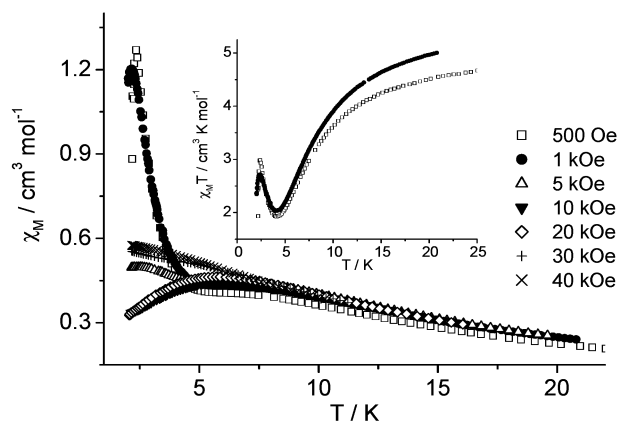
The field-dependent magnetization of **1** shows a pronounced sigmoid shape, indicating the occurrence of a magnetic transition from the nonmagnetic ground state to a spin-polarized state (Figure 5). The transition field, determined by  $dM/dH$  derivative curve, is ca. 25 kOe. This is further proved by the field-dependent ac magnetic susceptibilities (Figure 6). For the Co(II) ion in an octahedral environment, an  $S = 1/2$  ground state is commonly observed at low temperatures because of the overall effect of crystal field and spin–orbit coupling.<sup>3</sup> The magnetization at 70 kOe is 5.3  $\text{N}\beta/\text{Co}_2$  unit for **1**, higher than the saturation value of 4.6  $\text{N}\beta$  anticipated for a pair of  $S = 1/2$  spins with  $g = 4.6$ .<sup>24</sup> A similar field-induced magnetic transition has also been found in compound  $(\text{NH}_4)_2\text{Co}_2(\text{hedpH})_2$ , where the  $\{\text{Co}_2(\text{hedpH})_2\}_n$  chains are packed in such a way that each chain is surrounded by six equivalent neighbors.<sup>20</sup> The transition field in the latter case, however, is ca. 35 kOe.



**Figure 5.** Field-dependent magnetization of **1** at different temperatures.



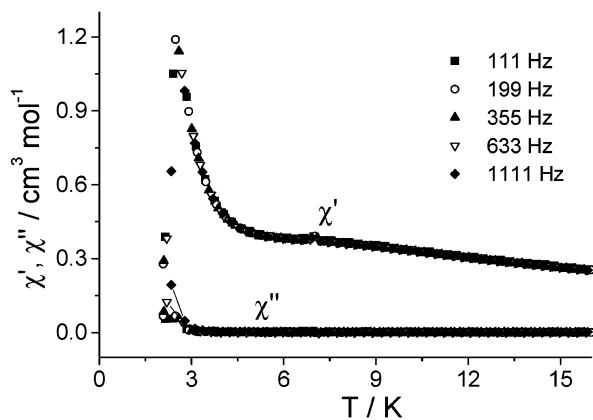
**Figure 6.** Field-dependent ac magnetic susceptibilities of **1** at different temperatures.



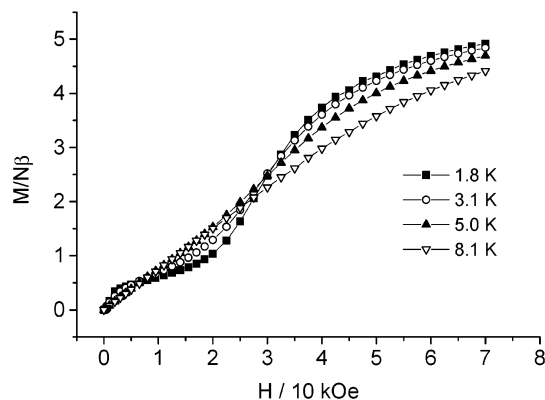
**Figure 7.**  $\chi_M$  vs  $T$  plots for **2** at different external fields. Inset:  $\chi_M T$  vs  $T$  plot at 500 Oe and 1 kOe.

Figure 7 shows the temperature-dependent molar magnetic susceptibilities of **2** at different external fields. At 500 Oe,  $\chi_M$  also passes through a broad maximum around 7 K, characteristic of a low-dimensional antiferromagnet. Near 4 K, however, the  $\chi_M$  value increases abruptly and reaching a maximum of 1.27  $\text{cm}^3 \text{mol}^{-1}$  at 2.3 K then drops quickly. The appearance of a sharp peak around 2.3 K is indicative of a long-range antiferromagnetic ordering. The  $\chi_M T$  vs  $T$  curve (see inset of Figure 7) shows that initially  $\chi_M T$  decreases continuously on cooling from 25 K until reaching a minimum of 1.92  $\text{cm}^3 \text{K mol}^{-1}$  at 4.1 K. Then it increases to a maximum of 2.98  $\text{cm}^3 \text{K mol}^{-1}$  at 2.4 K, followed by a drop toward zero. The upturn of  $\chi_M T$  below 4.1 K suggests

(24) Caneschi, A.; Dei, A.; Gatteschi, D.; Tangoulis, V. *Inorg. Chem.* **2002**, *41*, 3508.



**Figure 8.** Temperature-dependent ac magnetic susceptibilities of **2** under different frequencies.



**Figure 9.** Field-dependent magnetization of **2** at different temperatures.

an uncompensated magnetic moments of the system arising from spin canting of the antiferromagnetically coupled Co(II) ions. When the field is high ( $\geq 40$  kOe), both peaks in the  $\chi_M$  vs  $T$  curves disappear, suggesting the occurrence of field-induced magnetic transitions.

The zero-field ac susceptibility measurements performed in the range 5–16 K, at  $H_{ac} = 5$  Oe and frequencies of 111, 199, 355, 633, and 1111 Hz, show both in-phase [ $\chi_M'(T)$ ] and out-of-phase [ $\chi_M''(T)$ ] signals at ca. 2.5 K, in agreement with a canted antiferromagnet (Figure 8). No frequency dependence was observed, excluding any glassy behavior.

The field-dependent magnetization of compound **2**, measured at 1.8 K, shows a two-step field induced transition (Figure 9). From 0 to 5 kOe, the magnetization increases quickly reaching a saturation value of  $0.46 N\beta$  at 5 kOe, which is equivalent to 10% of that expected for ferromagnetic ordering. Above 5 kOe, a sigmoid shaped curve is found. Like compound **1**, this corresponds to the transition to a polarized state. The critical field, indicated by  $dM/dH$  curve, is 27.5 kOe at 1.8 K. The magnetization at 70 kOe is  $4.9 N\beta/\text{Co}_2$  unit for **2**, close to the saturation value of  $4.6 N\beta$  anticipated for a pair of  $S = 1/2$  spins with  $g = 4.6$ . The field-dependent ac magnetic susceptibilities result in the same conclusion (Figure 10).

Several cobalt phosphonates have been reported to be canted antiferromagnets including compound  $\text{Co}_3(\text{O}_3\text{PC}_2\text{H}_4-$

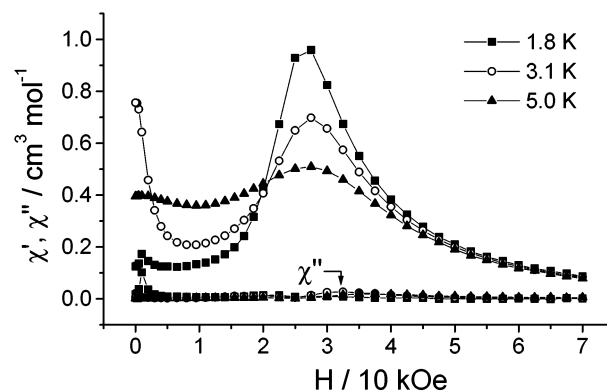


**Figure 10.** Field-dependent ac magnetic susceptibilities of **2** at different temperatures.

$\text{CO}_2)_2$  with a three-dimensional structure<sup>14</sup> and compound  $\{\text{K}_2[\text{CoO}_3\text{PCH}_2\text{N}(\text{CH}_2\text{CO}_2)_2]\}_6 \cdot x\text{H}_2\text{O}$  with a molecular structure.<sup>15</sup> The canting effect could be caused by the antisymmetric interactions related to the symmetry of the exchange pathways joining the magnetic centers, as well as the single ion anisotropy. Since both compounds **1** and **2** contain ladderlike chains of  $\{\text{Co}_2(\text{hedpH})_2\}_n$  in which the Co(II) ions through  $\mu\text{-O}(4)$  bridge are related by an inversion center, the observation of spin canting in compound **2** while not in compound **1** could be due to the structural phase transition in **2** at low temperature.

Previously, we reported the structures of three Mn analogous, measured at 223 K, with formula  $[\text{NH}_3(\text{CH}_2)_n\text{NH}_3][\text{Mn}_2(\text{hedpH})_2] \cdot 2\text{H}_2\text{O}$  [ $n = 4$  (**Mn-4**), 5 (**Mn-5**), 6 (**Mn-6**)].<sup>18</sup> It has been found that the structures of **Mn-4** and **Mn-6**, with even numbers of methylene groups in the dication chain, crystallize in the centrosymmetric space group  $P2_1/n$ , while **Mn-5** having an odd number of methylene groups crystallizes in the chiral space group  $P2_1$ . In the present cases, although the dication  $[\text{NH}_3(\text{CH}_2)_5\text{NH}_3]^{2+}$  in compound **2** is disordered at room temperature, the possibility of structural phase transition from achiral to chiral at very low temperature cannot be excluded.

In summary, this paper describes the syntheses and crystal structures of two new cobalt(II) diphosphonates:  $[\text{NH}_3(\text{CH}_2)_n\text{NH}_3]\text{Co}_2(\text{hedpH})_2 \cdot 2\text{H}_2\text{O}$  [ $n = 4$  (**1**), 5 (**2**)]. Both contain ladderlike chains with the same composition  $\{\text{Co}_2(\text{hedpH})_2\}_n$ . Each chain is strongly hydrogen bonded to its four equivalent neighbors, hence generating three-dimensional networks with channels where the diammonium counterions and lattice water reside. The magnetic behavior of compound **1** is typical for a low-dimensional antiferromagnet. The field-induced magnetic transition from the nonmagnetic ground state to a spin polarized state is observed with the critical field of ca. 25 kOe at 1.8 K. Such a behavior is reminiscent of a quantum spin system. For compound **2**, a similar field-induced magnetic transition is also observed at ca. 27.5 kOe at 1.8 K. In addition, compound **2** experiences long-range canted antiferromagnetism at very low temperature which could be explained by its structural phase transition at low temperature.

**Acknowledgment.** The authors thank the National Natural Science Foundation of China, the Ministry of Education of China, the Natural Science Foundation of Jiangsu Province, and the Analysis Center of Nanjing University for financial support and Mr. Yong-Jiang Liu for crystal data collection.

**Supporting Information Available:** X-ray crystallographic files, in CIF format, and additional figures for the two compounds. This material is available free of charge via the Internet at <http://pubs.acs.org>.

IC034614R